

## Supplementary Information

# Low-cost Electrochemical Paper-based Device for Exosome Detection

Surasak Kasetsirikul <sup>a,b</sup>, Kim Thinh Tran<sup>c</sup>, Kimberley Clack <sup>a,c</sup>, Narshone Soda <sup>a</sup>, Muhammad J. A.

Shiddiky <sup>a,c</sup>, Nam-Trung Nguyen <sup>a</sup>

<sup>a</sup> Queensland Micro-and Nanotechnology Centre (QMNC), Griffith University, Nathan Campus, Nathan, QLD 4111, Australia

<sup>b</sup> School of Engineering and Build Environment (EBE), Griffith University, Nathan Campus, Nathan, QLD 4111, Australia.

<sup>c</sup> School of Environment and Science (ESC), Griffith University, Nathan Campus, Nathan, QLD 4111, Australia

## S.1 Attenuation of DPV peak current from subsequent layer addition

The addition of stepwise biomolecular binding and subsequent layering at the electrode surface results in the attenuation of DPV current.

To assess the validity of antibody immobilization and stepwise surface blocking, we performed control experiments for monitoring the DPV current change under varying CD9 and BSA conditions as follows:

- 1) The DPV current change ( $\%I^{CD9}$ ) was measured in the presence of anti-CD9, and in the absence of anti-CD9.  $\%I^{CD9}$  measured in the presence of anti-CD9 is significantly higher than that of in the absence of anti-CD9 (17.23% versus 4.44%, respectively), Figure S1a.
- 2) The DPV current change ( $\%I^{BSA}$ ) was measured in the presence of BSA surface blocking and in the absence of BSA surface blocking.  $\%I^{BSA}$  is significantly higher than that of in the absence of BSA (14.68% versus 5.58%, respectively), Figure S1b. The RSD (relative standard deviation) was less than 10% ( $n = 5$ ). It is worth noting that subsequent washing or several treatment steps on the paper-based device may affect the conductivity of the electrode, resulting in decreased DPV peak current in every step.

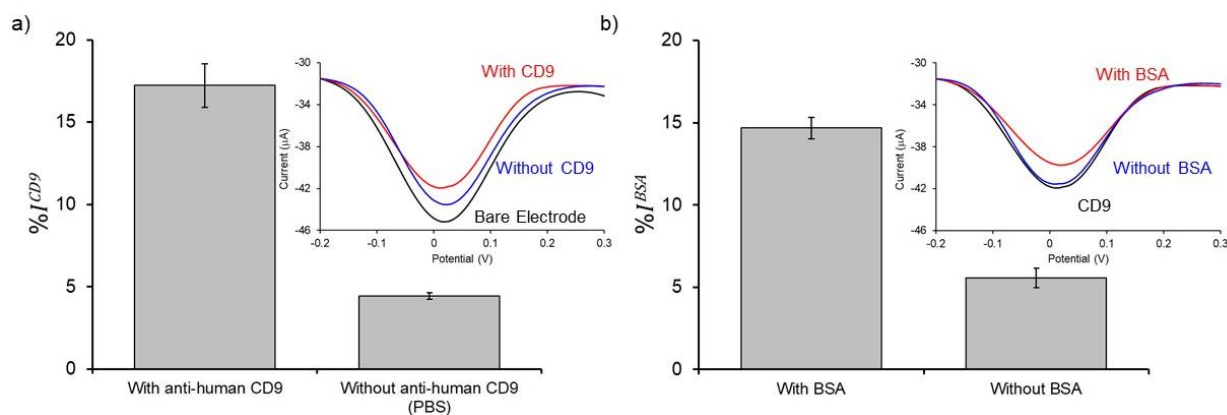


**Fig. S1.** a) Mean value for DPV current change  $\%I^{CD9}$  obtained in the presence and absence of anti-CD9 immobilization. Inset shows the corresponding DPV current response. b) Mean value for DPV current change  $\%I^{BSA}$  obtained in the presence and absence of BSA blocking. Inset shows the corresponding DPV signal changes in the presence and absence of BSA. Each data represents the average results obtained for five devices ( $n = 5$ ) and the error bars represent the standard deviation for five individual replicates.

## S.2 Electrochemical Impedance Spectroscopy (EIS)

The successful binding of anti-CD9, CA125 (+) OVCAR3 exosomes and anti-CA125, on 3-carbon electrode paper-based devices was observed by EIS (Fig. S2). The assay complex hinders the interfacial electron transfer reaction of the  $[\text{Fe}(\text{CN})_6]^{3-/4-}$  redox reaction. The electron-transfer process is determined by the semicircle range observed at higher frequencies in Nyquist plot. Thus, electron transfer resistance ( $R_{\text{et}}$ ) corresponds to the diameter of semicircle region. We observed an increase of electron transfer resistance ( $R_{\text{et}}$ ) resulting from the addition of subsequent biomolecules on electrode surface (Fig. S2a). The red colour curve indicates the baseline from PCEs, giving the lowest semicircle domain determining the fastest electron transfer.  $R_{\text{et}}$  was increased after incubating 0.1 mg/mL anti-human CD9 for 20 min in blue colour, blocking with 2% BSA for 20 min in violet colour, capturing  $2.47 \times 10^9$  exosome/mL of CA125(+) OVCAR3 exosomes for 30 min in green colour, and detecting 50  $\mu\text{g/mL}$  anti-CA125 for 30 min in navy colour, which presents larger semicircle domain depending on subsequent additions of biomolecules. However, when the exosome sample was replaced by control sample (PBS), the semicircle region (yellow line and orange line, which are control sample (PBS) and 50  $\mu\text{g/mL}$  anti-CA125, respectively) does not become larger with the subsequent addition due to non-specific binding as compared to the CA125(+) OVCAR3 exosomes sample and anti-CA125, respectively (Fig. S2b). The EIS result also corresponds to the DPV experimental result to affirm the assay specificity of this PCEs device.

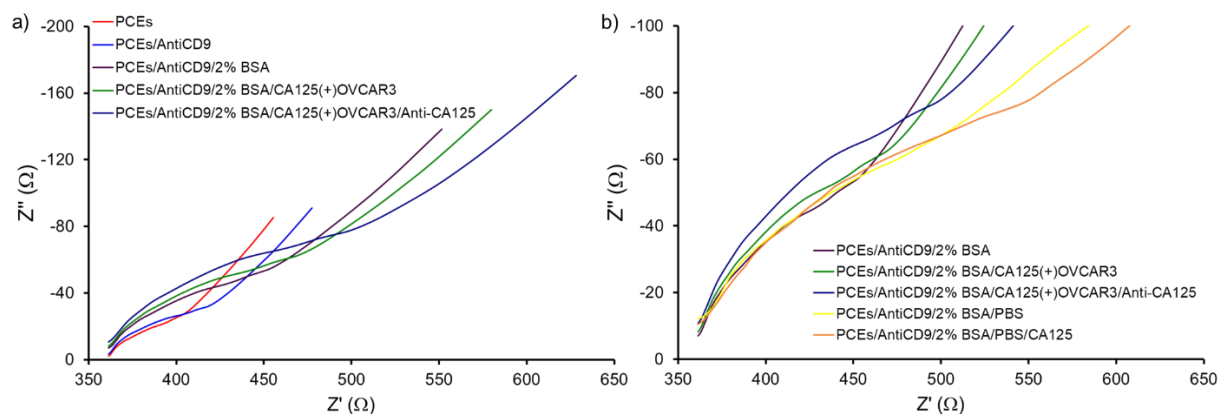


**Fig. S2.** a) Nyquist plots for an immunological assay with CA125(+) OVCAR3 exosome sample on PCEs for bare electrode (PCEs, red) and modified electrodes for detection (PCPs/anti-CD9, blue), (PCEs/anti-CD9/BSA, violet), (PCEs/anti-CD9//BSA/ CA-125(+)) OVCAR3 exosomes, green), and (PCEs/anti-CD9//BSA/ CA-125(+)) OVCAR3 exosomes/anti-CA125, navy) in PBS containing 5 mM  $[K_3Fe(CN)_6]$  and  $[K_4Fe(CN)_6]$  electrolyte solution b) Nyquist plots for an immunological assay with control sample (PBS) on PCEs (PCEs/anti-CD9//BSA/PBS, yellow) and (PCEs/anti-CD9//BSA/PBS/CA125, orange) in PBS containing 5 mM  $[K_3Fe(CN)_6]$  and  $[K_4Fe(CN)_6]$  electrolyte solution